IN_{avg} profile. As shown in Fig. 8D, the density interval within which this gradient occurs is characterized by the presence of the DCML, suggesting that the rapid decrease in nutrient concentrations measured at the IN-stations might be a direct result of an increased nutrient uptake associated with the higher concentrations of phytoplankton that characterize *Opal*'s core region (see Rii et al., 2008 for more details). The OUT_{avg} profile of chlorophyll *a* concentration indicates quite typical values for the region with a DCML concentration on the order of 0.4 mg m^{-3}, and the DCML depth located at about 120 m (e.g., Falkowski et al., 1991). As already noted, the IN_{avg} profile reveals that the DCML shoals upward to depths between 60 and 70 m at the center of the eddy, and average chlorophyll *a* concentrations almost double, reaching values above 0.7 mg m^{-3}.

Consistent with the vertical profiles shown in Fig. 4, 1000-m vertical profiles of dissolved oxygen (Fig. 8E) indicate that the eddy-induced uplift of isopleths extends down to depths between 600 and 700 m. The oxygen profiles are characterized by a homogeneous and relatively well oxygenated surface layer through the upper 200 m. Below, there is a region where oxygen concentrations decrease quite sharply to values of roughly 6 mg L^{-1}. Comparison of Fig. 8E with Fig. 4C clearly indicates that the oxygenated surface layer corresponds to the upper mixed layer, and that this layer is much shallower at the IN-stations because of the eddy-induced uplift. Most importantly, the IN_{avg} profile shows that a much steeper gradient toward low oxygen values occurs at depths just below the DCML, as also indicated by the sharp decrease in oxygen concentrations between the $\sigma-t_{24}$ and $\sigma-t_{24.5}$ levels in Fig. 8F. As mentioned above in the discussion of the dissolved oxygen sections shown in Figs. 6 and 7, this observation suggests increased oxygen consumption, which is most likely caused by enhanced remineralization at the center of the eddy below the DCML.

3.3. ADCP data

ADCP velocity vectors at 40 m depth for Transects 3 and 4 are shown in Fig. 9, clearly revealing a velocity field dominated by the presence of the strong cyclonic flow associated with Cyclone *Opal*. The positions of the center of the eddy are approximately

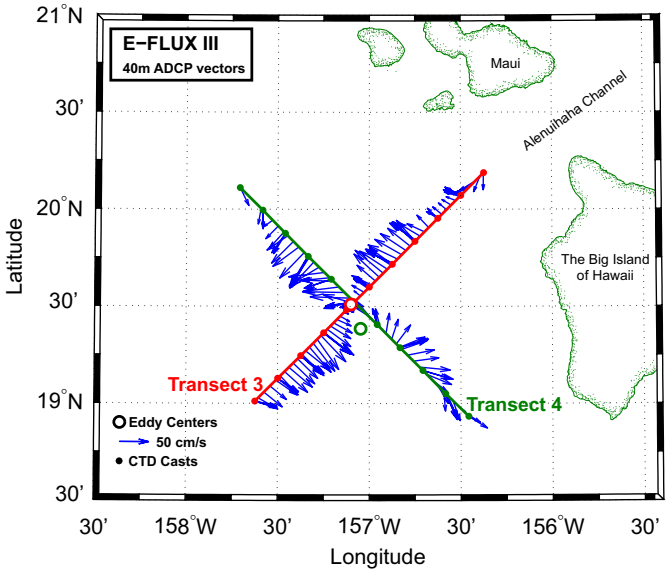

Fig. 9. The 40 m ADCP vectors for Transects 3 and 4. The dots indicate the locations where CTD casts were made. The two circles indicate the best estimated positions of the center of Cyclone *Opal* for the two transects.

indicated in both transects by the areas of minimum velocity. Velocities gradually increase with radial distance from those areas before peaking and then slowly decaying. The fact that during Transect 3 the velocity vectors were almost perpendicular to the transit track, changing direction after having fallen to near zero values, indicates that this section passed very near to *Opal*'s center. By comparison, Transect 4 did not pass as close to the center; this transect likely crossed the eddy a few km to the east of its center according to the ADCP data as well as CTD and biogeochemical data discussed above. The presence of multiple velocity values sampled at each hydrographic station results from the relatively long time interval required to perform a CTD cast (usually 45–60 min) compared to the ADCP sampling interval (15 min, see Dickey et al., 2008). The several velocity measurements collected at each CTD cast location were replaced with their mean value before ADCP data were analyzed. The resulting velocity records were characterized by a more regular spatial distribution of the data along each transect. This characteristic was particularly important to prevent the occurrence of anomalously large values when horizontal gradients of velocity were computed.

Due to the cyclonic nature of the velocity field, the analysis of *Opal* dynamics is conducted using cylindrical coordinates, and the recorded zonal and meridional velocities are decomposed into radial and tangential components. The origin of the reference system is centered at the eddy's center, so that in order to convert the velocity field into cylindrical coordinates, the first step was to accurately locate the position of the center of the eddy at every depth for the two transects. An area of about 30 × 30 km around the minimum velocity zone of each transect was divided into a grid of 30 × 30 points. ADCP velocities were decomposed into tangential and radial components relative to each point of the grid, so that every point of the grid was tested as a possible location for the center of the eddy. At every depth the center of the eddy was best estimated as the grid point for which the mean tangential velocity computed from the 25 nearest ADCP records was maximal. The decision of using only the 25 nearest velocities was made so that the location of the center was not affected by the peripheral regions where the cyclonic flow associated with *Opal* became more perturbed due to the growing influence of the outer velocity field.

Fig. 10 shows the 40 m depth positions of the center of *Opal* as computed for Transect 3 (A) and Transect 4 (B). In each figure the contour plot defines the area where the 30 × 30 points grid was defined, and isopleths indicate equal values of the mean tangential velocity associated with each grid point. The ADCP velocities used to determine the eddy center position are shown as blue vectors. Clearly the two figures confirm that Transect 3 crossed Cyclone *Opal* almost exactly at its center, whereas during Transect 4 the center of the eddy was a few km to the west of the transit track. Variations of the position of the center with depth are much less pronounced for *Opal* than for E-Flux I Cyclone *Noah* (see Kuwahara et al., 2008). For this reason the center position determined at the 40-m depth can be taken as a good approximation of the center position throughout the whole water column.

The center of the eddy also could have been best estimated as the grid point at which radial velocities are minimized. More precisely, the center of the eddy could have been located at the grid point for which the root mean square of the radial velocities is minimal. However, since radial velocities within the eddy are usually much smaller than tangential velocities, and therefore more sensitive to the variations associated with background noise, the center positions found using this method were considered to be less accurate. It is important to emphasize that differences between the two methods are usually relatively small and that the